

Laser based foil rear side metallization for crystalline silicon solar cells

Jan Nekarda, Martin Graf, Andreas Rodofili, Andreas Wolf, Ralf Preu

Fraunhofer Institute for Solar Energy Systems (ISE), Heidenhofstrasse 2, 79110 Freiburg i.
Breisgau, Germany

Phone: +49 (0)761-4588-5479, Fax: +49 (0)761-4588-7812, e-mail: jan.nekarda@ise.fraunhofer.de

ABSTRACT

In this contribution we present different results of our investigations regarding the use of aluminum foil as rear side metallization for solar cells with dielectric passivation and laser fired contacts (LFC). We investigate the impact of different laser processes on the resistance of the contacts, the adhesion properties of the foil and the efficiency potential. By fabricating highly efficient, $20 \times 20 \text{ mm}^2$ sized solar cells with a conversion efficiency of 21.0 %, we demonstrate the high potential of this approach, which is equal to that of LFC-cells with common screen-printed or PVD metallization on the rear side. We investigated the optical properties of such metallized rear sides which benefit from an embedded air gap between foil and passivation layer. Finally, we present first solar cell results on industrially sized wafers ($A=238 \text{ cm}^2$) demonstrating again the equal efficiency potential compared to PVD metallization.

Keywords: Laser Processing, Manufacturing and Processing, Metallization, Contacting

1. INTRODUCTION

To make solar energy competitive in the long run, the price per watt-peak has to decline. Therefore, new cell concepts, with higher efficiency and cost saving potential have to be introduced into the market. Laser firing of local contacts (LFC) [1] is a promising technique which allows the use of dielectrically passivated rear sides as introduced by Blakers *et al.* [2] with the passivated emitter and rear cell (PERC) already more than 20 years ago. In this approach, the aluminum is contacted with the silicon through the dielectric passivation by means of single laser pulses. The potential of this cell type has already been proven and first companies have adopted this technology in their production facilities recently. As the metallization is the main cost driver in cell production, the LFC approach features high saving potential since it enables the use of aluminum foil as rear side metallization [3]. The foil is fused to the wafer during the contacting process and thereby replaces conventional metallization processes, such as screen printing or physical vapor deposition (PVD). Besides the cost saving potential, it yields other advantages like minimum thermal and mechanical impact or the possibility to use new interconnection approaches.

In this paper we present a comparison of different laser processes regarding the resistance of the contacts their adhesion properties and efficiency potential. We evaluate the potential of this approach by processing highly efficient solar cells and compare them with conventionally metallized cells with LFC contacts which feature either screen printed or PVD metallization. Finally, we present the optical properties of such metallized rear sides and present the first solar cell results on large silicon substrates ($A=238 \text{ cm}^2$).

2. PROCESS SEQUENCE

Since the foil is fixed onto the wafer during the LFC contacting process, it is rolled over the rear side before the laser process. In order to achieve sufficient contact quality, the foil has to lie on top of the wafer as close as possible during laser processing to allow the formation of an aluminum-silicon connection. This connection does not only form the electrical contact but also leads to the relevant adhesion of the foil. If the foil is not attached properly during the laser process, a simple perforation of the foil takes place and neither an electrical, nor a mechanical connection is formed.

Hence, the spreading of the foil is a critical process step. A sufficiently close contact between foil and wafer can be achieved by sucking the foil onto the substrate. The whole procedure of applying the foil and fixing it by laser irradiation has been patented by Fraunhofer ISE [4].

3. EVALUATION OF DIFFERENT LASER PROCESSES

3.1 Resistance of point contacts

Beside the right setup, the laser process is crucial for this application. Therefore, we compared two different IR lasers with similar pulse energies but a different pulse length regime. Process “A” consists of a multi pulse process with short pulse lengths whereas process “B” is a single pulse process with similar total laser energy per contact but longer pulse duration. The peak irradiation intensity of both laser processes varies by two orders of magnitude which leads to different contact formation processes as can be seen from microscope images of the contacts in figure 3. The picture of a contact formed by process “A” (left) shows a significant melt ejection, which attests a high process dynamic whereas process “B” (right) seems to be based on “smoother” melting.

After identifying adequate parameter ranges for both laser processes regarding the foil adhesion issue, we determined the resistance of a single contact R_{LFC} . We used samples with a defined base resistivity ρ of 1 Ωcm and a stack of Al_2O_3 and SiO_x as passivation on one side; both deposited by means of plasma enhanced chemical vapor deposition (PECVD). The other side receives a full area contact by screen printing metallization and subsequent firing. Finally, the foil is fixed onto the passivated side with a defined amount of contacts N_c by means of different laser processes. The series resistance of the sample can be measured as schematically shown in Figure 1.

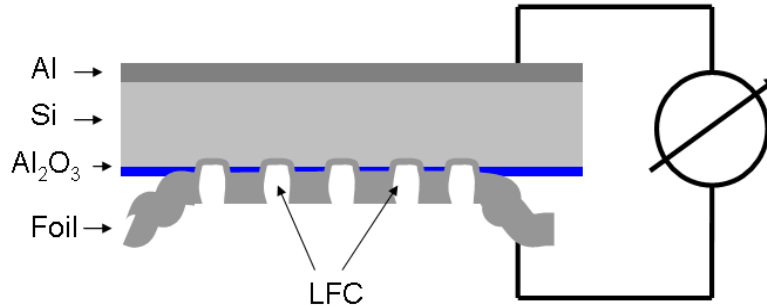


Figure 1: Sketch of the resistivity measurement of a defined number of LFC contacts.

Consequently, the resistance of one contact can be determined by measuring the series resistance of the sample before ($R_{s,1}$) and after the LFC process ($R_{s,2}$) and using equation (1) regarding the offset (os_{me}) of the measuring equipment.

$$R_{LFC} = \frac{N_c}{(R_{s,2} - os_{me})^{-1} - (R_{s,1} - os_{me})^{-1}} \quad (1)$$

The determined values R_{LFC} are 49.5 Ω (process “A”) and 149 Ω (process “B”). Assuming a radius $r_{LFC} \approx 48 \mu\text{m}$, which is in good agreement with the microscope image for contacts “A”, the resistance R_{LFC} matches the value of the so called spreading resistance which can be calculated, considering the radius of the contacted area r_{LFC} , the wafer thickness W ($W = 250 \mu\text{m}$) and the base resistivity ρ ($\rho = 1 \Omega\text{cm}$), by a formula derived by Cox and Strack [5] (equation 2).

$$R_{spr} = \frac{\rho}{2 \cdot \pi \cdot r_{LFC}} \cdot \arctan\left(\frac{2 \cdot W}{r_{LFC}}\right) \quad (2)$$

In case of process “B” the higher resistance indicates a smaller radius of $r_{LFC} \sim 17 \mu\text{m}$ according to equation (2). The microscope image in figure 3 denotes a larger area but this is not significant, since it only shows the top of the aluminum foil. Due to the smooth laser process the molten area at the opposed surface of the foil and consequently the contacted area results to be smaller (see figure 2, below). Here the same contact as shown in figure 2 on the left side above is pictured after removing the foil. However, when processing solar cells the measured resistance is taken into account to calculate the optimum contact pattern.

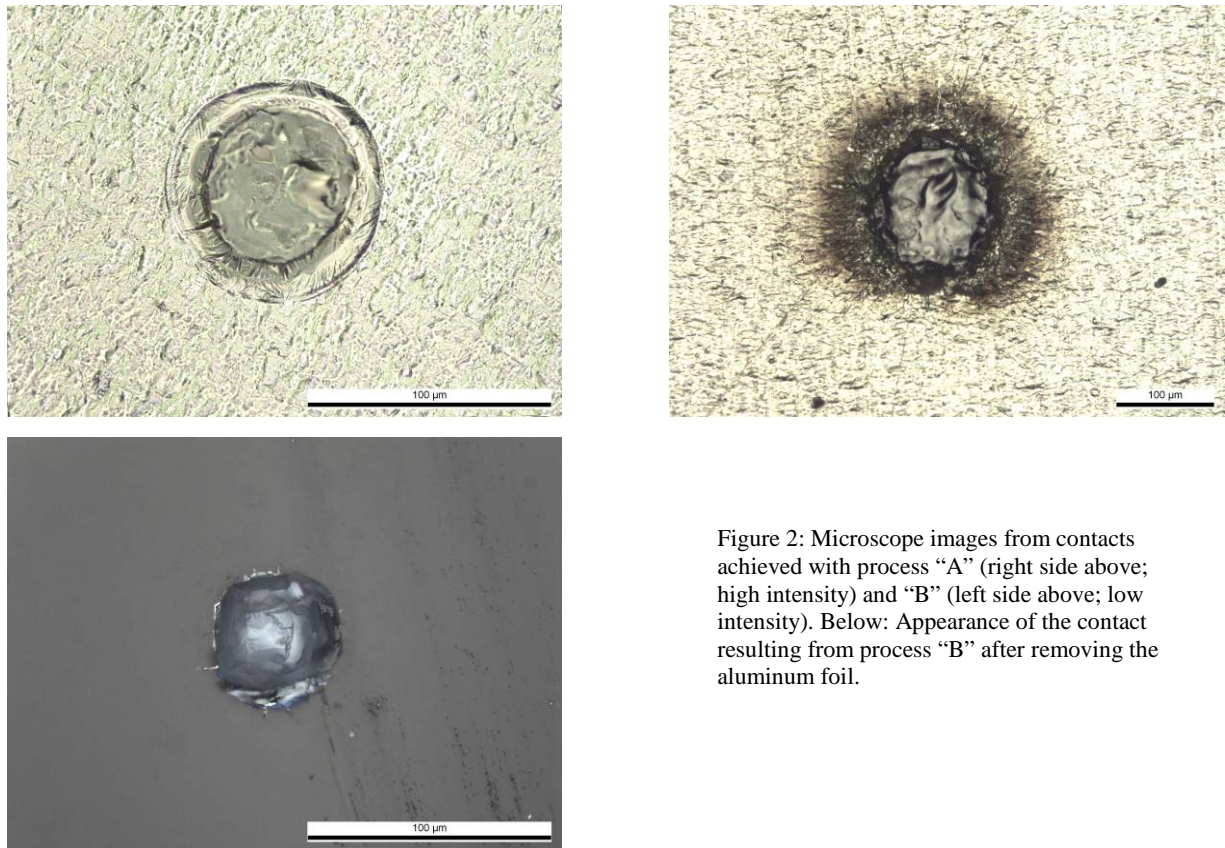


Figure 2: Microscope images from contacts achieved with process “A” (right side above; high intensity) and “B” (left side above; low intensity). Below: Appearance of the contact resulting from process “B” after removing the aluminum foil.

3.2 Adhesion properties

The adhesion of the layer is a crucial quality feature of any metallization concept. To determine reliable values, we used eight $5 \times 5 \text{ cm}^2$ sized test samples consisting of industrial mono-crystalline silicon wafers deposited with a 100 nm thin passivation layer of SiO_2 . Before the oxidation, the wafer underwent the usual chemical cleaning sequence but the surface was not treated in any special way like grinding or polishing. The samples were covered with foil on a $4 \times 4 \text{ cm}^2$ sized area using both laser processes “A” and “B” with different contact pitches L_p leading to different coverage fractions f between 0.2 - 3 %. The latter is calculated assuming r_{LFC} values as predicted from the measured contact resistance and equation (2) with L_p being the pitch equivalent to a quadratic pattern by:

$$f = \frac{r_{LFC}^2 \cdot \pi}{L_p^2} \quad (3)$$

In PERC devices, common values of the coverage fraction f are in the range of 1-2 % depending mainly on the base resistivity ρ of the used silicon material. We fixed a 30 mm wide stripe of special tape onto the foil as shown in the right picture of figure 3 while the tape has no contact to the wafer anywhere beside the foil. The tape is also used to fix the sample on the table of a special measurement tool which is usually used to determine the adhesion of interconnection bands (see figure 3, left). During the measurement procedure, the force is logged while slowly pulling off the foil over a distance of ~ 30 mm at an angle of 90°.

In figure 4, a characteristic progression of the peeling force is shown for a sample where laser process “B” with a coverage fraction of $f = 0.74$ % is used. The required peeling force for a 30 mm wide stripe of foil is in the range of a few Newton.

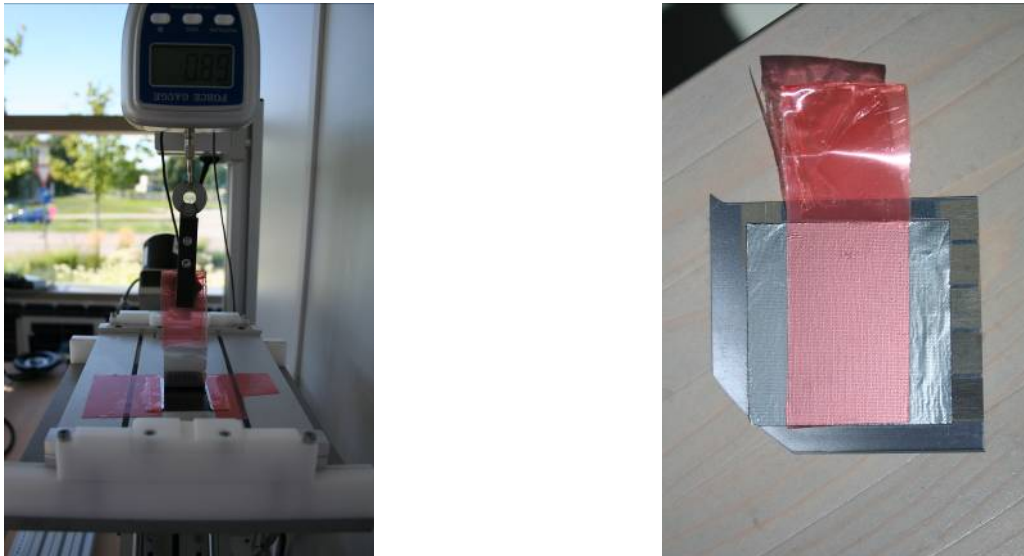


Figure 3: prepared sample with a 30 mm wide tape (right) and the used “peel-off” force measuring tool at the Fraunhofer ISE module technology center (left)

At the beginning of the measurement sequence the tape has to be tightened and the force rises until a maximum value where the foil at both edges of the tape rips (see figure 4, left). At all investigated coverage fractions, the adhesion of the foil is strong enough that the foil rips of directly at the edge of the pulling tape as seen in figure 3 (left). Therefore, it is justifiable that the measured peeling force always contributes to a 30 mm wide stripe of foil. Subsequently, the force drops to a characteristic level over the remaining peeling distance until the whole stripe is removed. To compare adhesion properties which are achieved by different laser processes and to evaluate the influence of the coverage fraction, we averaged the measured data over the characteristic plateau behind the first peak. In figure 5 these values are plotted against the coverage fraction for both processes. Although the amount of data is too little for a strong proof of linear correlation the expected dependence between both values is observed.

The contacts made with process “B” clearly achieve a better adhesion compared to process “A” since the peeling force is higher at equal contacting area ratio. An adhesion force of 1 N per mm width of the interconnection ribbon is the requirement for module manufacturer. Hence, solar cells featuring such rear side foil metallization cannot be interconnected using the conventional soldering procedure. However, if interconnection is applied over a wider area, adhesion is strong enough to guarantee a solid interconnection even if legal requirements are not complied.

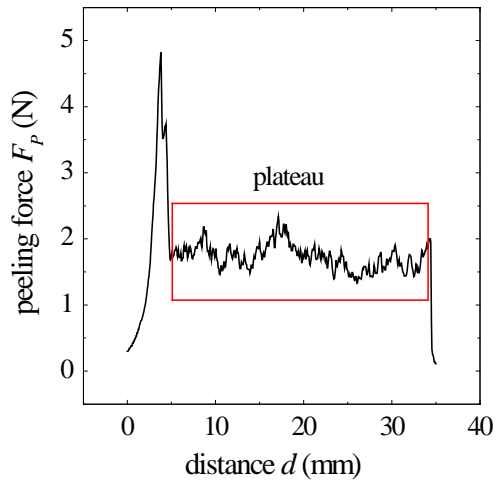


Figure 4: Required peeling force to remove a 30 mm wide stripe of foil, which is fixed to the wafer with process “B” applying a contact distance L_p of 350 μm and respectively a coverage fraction of 0.74 %, leading to an average peeling force of $F_p = 1.8$ N.

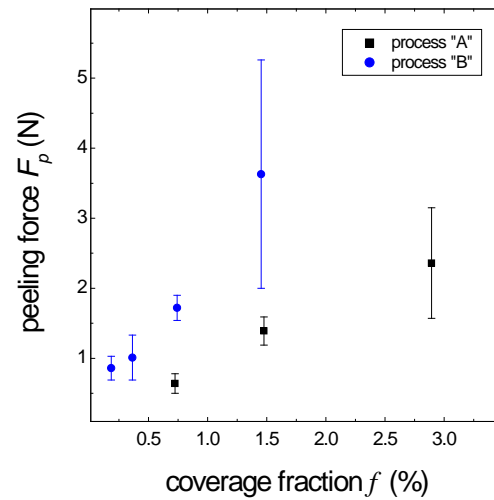


Figure 5: Peeling forces for a 30 mm wide stripe of foil in dependence of the used laser process and LFC contact coverage fraction.

3.3 Evaluation of the efficiency potential of laser processes “A” and “B”.

In order to investigate the influence of the different laser processes we fabricated highly efficient solar cells. We used 4 inch float zone wafers with a thickness of $W=250$ μm and a base resistivity of $\rho=1$ Ωcm . Each wafer contains seven 2×2 cm^2 sized cells, featuring random pyramid texturisation and a shallow 110 Ω/sq . emitter. This is covered by a 70 nm thin PECVD deposited silicon nitride SiN_x layer providing emitter passivation as well as anti-reflection properties. The front side is contacted by fine line aerosol printing [6], which was fired and subsequently electroplated with silver [7]. The rear side contains a 10 nm thin atomic layer deposited (ALD) aluminum oxide Al_2O_3 which is covered by 90 nm of PECVD deposited silicon oxide SiO_x . For rear side metallization, we used an 8 μm thin foil which is connected by the different laser processes with the corresponding contact pattern. For all the fabricated highly efficient solar cells no tempering after LFC was carried out. The process sequence is shown in Figure 6 (foil) in the next section. In Table 1 (also next section) the results of the I-V measurements are listed.

The mean value considers seven cells from the best wafer. It can be clearly seen that:

1. Laser process “A” leads to a significant higher open circuit voltage of about 10 mV.
2. Due to the longer pulse duration Process “B” forms a significantly deeper region with aluminum-silicon alloy underneath the contact. This region seems to have a much higher recombination of charge carriers.
3. The similar fill factors FFs show that the contact pattern was chosen right regarding the different resistances of the contacts of both processes. Therefore the loss in voltage of process “B” cannot be explained by a too large contact fraction on the rear side.
4. With the multi pulse process “A” an efficiency of 21.0 % could be reached with the best cell.

4. COMPARISON OF DIFFERENT METALLIZATION TECHNOLOGIES

4.1 Evaluation of the efficiency potential.

To benchmark the efficiency potential of the foil approach, we have additionally processed high efficiency solar cells featuring screen-printed and evaporated rear side metallization within the former solar cell batch (see section 3.3). All rear sides have been passivated by 10 nm thick atomic layer deposited (ALD) aluminum oxide Al_2O_3 . This is covered by a PECVD deposited layer of silicon oxide SiO_x in case of PVD metallization. The screen printed cells received a capping layer of SiN_x instead, which also was deposited by means of PECVD. As metallization we either used 6 mg/cm^2 screen print paste, or $2 \mu\text{m}$ thin PVD aluminum, which was evaporated on an industrial pilot line machine [6]. For PVD metallized surfaces a single pulse LFC process was used, whereas on screen printed rear sides a different multi pulse process was applied. Again, the contact pattern was adapted to the resistance of the respective point contacts and no tempering was performed after LFC processing. The process sequence is shown in Figure 6. The results of the I-V measurement are shown in Figure 9 and listed in Table 1.

Regarding the open circuit voltage V_{oc} , the PVD process yields the highest potential. Compared to the foil approach this is likely due to the single pulse laser process. Although the screen printed approach should also suffer from increased laser damage, an additional contribution could possibly arise from the different passivation. However, the outlier shows that the same high voltage level, compared to PVD metallization, is achievable. It is noticeable that the short circuit current density J_{sc} is slightly increased in the case of the foil metallization. This could result from the slightly higher reflectance of these rear sides in the long wavelength range which is discussed in the next section. The fill factor is at an equal level, which indicates that the corresponding contact pitch, or respectively the coverage fraction, is well chosen for the different laser processes. However, the standard deviation of the fill factor in case of the PVD rear side is higher, which can be attributed to finger disruption, which were observed on the front side.

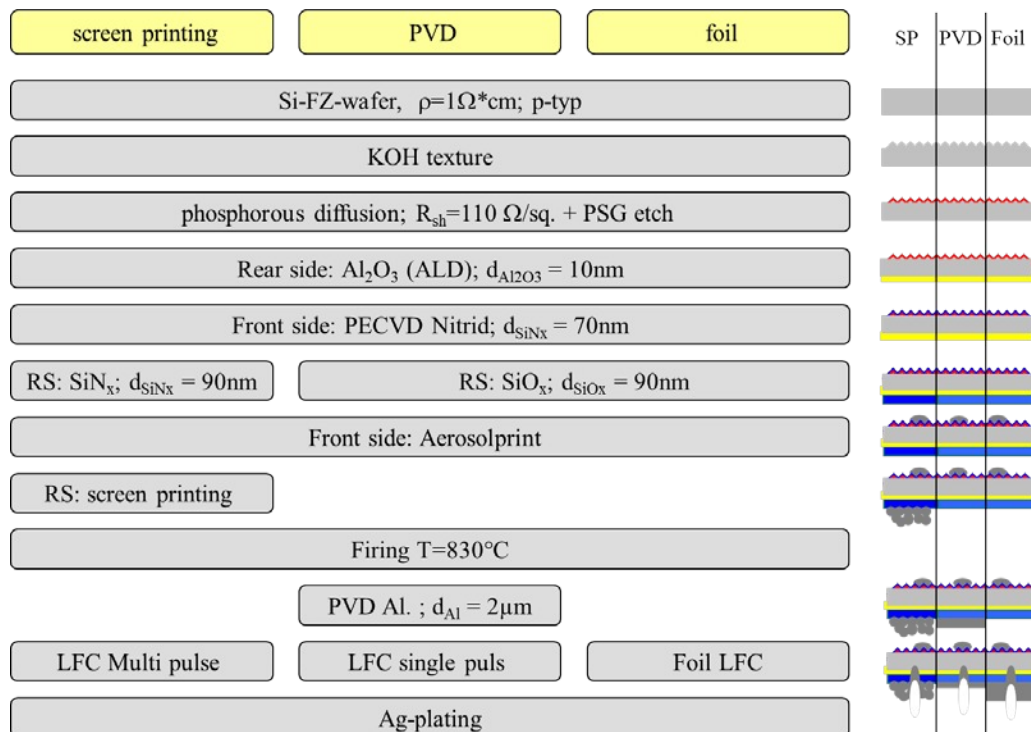


Figure 6: Process flow (left) and schematic cross section (right) of highly efficient solar cells with different rear side metallization approaches and laser fired contacts (LFC).

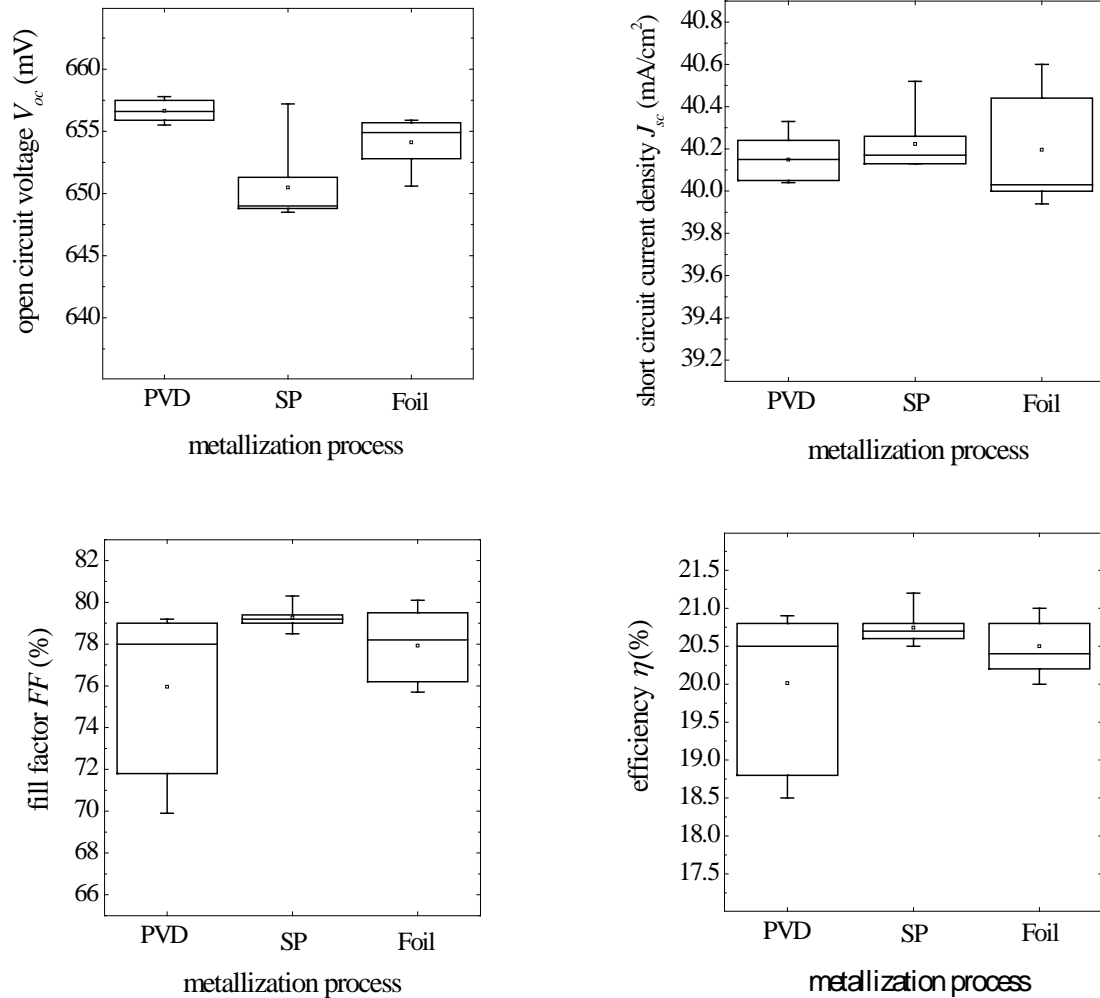


Figure 7: Analysis of the different I-V measurement parameters V_{oc} , J_{sc} , FF and η of seven highly efficient solar cells in dependence of the different used rear side metallization concept, using statistic box diagrams.

The overall solar cell efficiencies of all metallization concepts are on a comparable level. More detailed information would require a better statistics. Although the screen printing approach obtained the highest efficiencies, one has to consider that this is an outlier value. Additionally, this is in contrast to other publications [6].

Overall such similar efficiency potential is remarkable when considering the substantial differences in the metallization and laser processes. It points out the flexibility of the laser fired contact process, which can be adjusted to a wide range of metal layers offering a constant efficiency potential of above 20.5%.

Table 1: Results of the I-V measurements of highly efficient solar cells, which received rear side metallization by physical vapor deposition (PVD), screen-printing (SP) and foil metallization (foil). In case of foil metallization two different laser processes “A” and “B” were used. Shown are the mean and the best value out of seven cells.

Process	V_{OC} [mV]	J_{SC} [mA/cm ²]	FF [%]	η [%]
PVD				
mean	657 ± 0.9	40.1 ± 0.1	76.0 ± 3.7	20.0 ± 1
best	658	40.1	79.2	20.9
SP				
mean	651 ± 3.1	40.2 ± 0.1	79.3 ± 0.5	20.7 ± 0.2
best	657	40.1	80.3	21.2
Foil “A”				
mean	654 ± 2	40.2 ± 0.3	77.9 ± 1.8	20.5 ± 0.4
best	656	40.0	80.1	21.0
Foil “B”				
mean	645 ± 3.4	40.0 ± 0.2	77.4 ± 1.9	20.0 ± 0.4
best	648	40.1	78.5	20.4

4.2 Overall comparison

In terms of passivated rear sides with laser fired contacts, the use of screen printing technology represents a solution which is already transferable to industrial production. Equipment is widely available and currently used printing, firing and laser processes are approved. In addition, conventional module interconnection can be applied. Along with screen printed front side contacts, no limitations are caused by that approach. The development of new screen printing pastes and firing conditions, which are designed for that special purpose, still hold some potential for further efficiency progress of solar cells. Nevertheless, the cost saving potential is assumed to be comparably small, since the consumption of energy and paste will not be reduced substantially.

Regarding physical vapor deposition, the experience there is substantially well-founded since this technique is established for many years. Even when this experience was gained by using PVD laboratory systems, first results have shown that these processes can be transferred successfully to pilot line machines with an industrially suitable throughput [6].

Until new front side metallization concepts are introduced and as long as wafer thickness remains the same, one will hardly benefit from lower process temperature and reduced mechanical stress impact. Additionally, the remaining interconnection problem still has to be solved. However, the cost saving potential compared to screen printing can be substantial, since the cost of the aluminum foil consumption per wafer is in the range of ≈ 1 €.

The use of metal foil as rear side metallization is the least investigated approach and therefore only little experience exists. Additionally, no supplier offers any equipment or consumer goods so far and new procedures have to be developed for module interconnection of such cells. Nevertheless, this concept features the highest cost saving potential since the required foil per wafer costs are ≈ 0.5 €, assuming a cut-off of 50 % and no expensive vacuum technology or any energy intensive processes are necessary. Additionally, like PVD, this concept fulfills all needs that are addressed to future deposition procedures such as low temperature and mechanical stress impact. A summary of these different advantages and disadvantages is listed in table 2.

Table 2: Summarized advantages and disadvantages of each rear side metallization approach - screen printing (SP), physical vapour deposition (PVD) and foil - regarding their use for solar cell concepts with dielectric passivation and laser fired contacts. (*denotes vague assumptions, since no industrial equipment and process exists so far)

Issues	PVD	Screen Print	Foil
η -Potential	high	high	high
Flexibility	medium	low	high
Maturity	high	high	low
Metallization-process Temp.	~300°C	800-900°C	-
Stress impact	low	high	low
Inter-connection	not published	soldering	-
Equip. Suppliers	few	many	-
Equip. Investment	high	medium	*low
Operating Cost	medium	high	*low

5. INVESTIGATIONS REGARDING THE OPTICAL PROPERTIES OF FOIL METALLIZED REAR SIDES.

The first solar cells which were metallized with the foil approach used a SiO_2 -passivation and suffered from low values of V_{OC} . We suspect a thin air gap between passivation and aluminium which prevents the so called al-neal process to take place [8]. This process describes an increase in passivation quality, which is caused by the creation of hydrogen, which is generated by the dissociation of water at the interface of the passivation layer and the oxidizing aluminium layer. This air gap would also affect the optical properties, in detail the internal reflection at the rear side, which is relevant for incident light of wavelengths above 900 nm. To investigate the hypothetic embedded air gap, we simulated the influence with the program *Sunrays* [9] for a wavelength range between $900 \text{ nm} < \lambda < 1200 \text{ nm}$ for a $250 \mu\text{m}$ thin silicon wafer, which is passivated by Al_2O_3 and subsequently metallized with an $8 \mu\text{m}$ thick aluminum foil. We calculated the reflection in case of a 100 nm thin passivation layer for different thicknesses of the embedded air gap, between $0\text{-}1\text{mm}$ (see Figure 9, above). One can see that the internal reflection increases for all kinds of air gap from $\lambda < 1000 \text{ nm}$ on as it is well known. At higher wavelength the internal reflection increases stronger, if more air is embedded between passivation and foil.

Afterwards, we calculated the influence of the aluminum oxide layer thickness, which is varied between $1 \text{ nm} < W_{\text{Al}_2\text{O}_3} < 100 \text{ nm}_{\text{and}}$ in case of a $1 \mu\text{m}$ thin air gap (see figure 9, right), and without embedded air (see figure 9, below). It can be observed that the thickness of the aluminium oxide layer is not relevant any more concerning the optical properties of the rear side, if a thin layer of air is embedded between passivation and foil.

To verify the simulation results, we subsequently processed samples with a SiN_x anti-reflection-coating on the front side and Al_2O_3 layer with different thicknesses between $7\text{-}100 \text{ nm}$. We metallized one half of the batch with PVD aluminium and applied the LFC process. The other half was metallized by our foil process where we used the same contact pattern. Afterwards the internal reflection was measured at all samples. The results are shown in Figure 10.

It can be clearly seen, that in case of a $2 \mu\text{m}$ PVD metallization the optical properties depend strongly on the thickness of the underlying passivation layer. The internal reflection drops substantially with decreasing layer thickness. In case of the foil metallization, this behavior does not appear. According to the earlier simulations this can be explained by a layer of embedded air, which is located between passivation and foil and which is approximately less than 10 nm thick. Consequently, this layer allows for much thinner passivation layers and therefore can further decrease production costs.

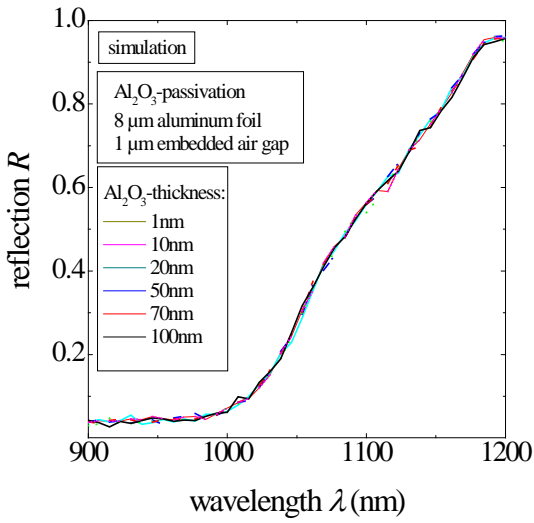
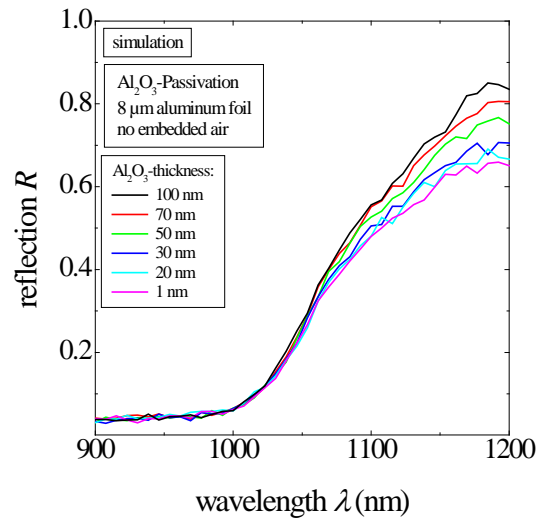
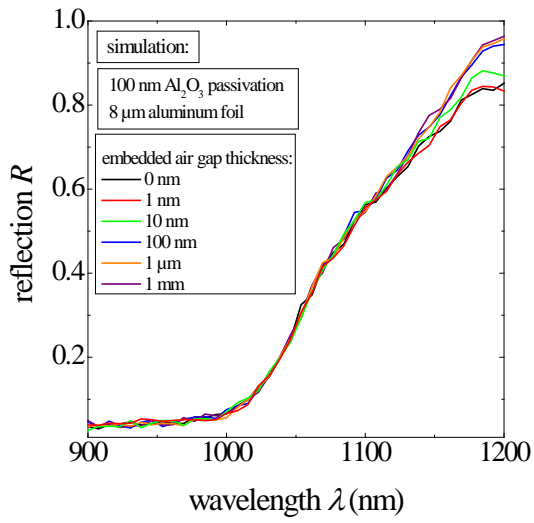


Figure 8: With the simulation program “Sunrays” calculated internal reflection characteristic ($900 \text{ nm} < \lambda < 1200 \text{ nm}$) on the rear side of a $250 \mu\text{m}$ thick silicon wafer. We assumed a layer stack consisting of $250 \mu\text{m}$ silicon bulk, aluminum oxide of different thickness in case of embedded air (right), and without air (middle) and a 100 nm thin Al_2O_3 layer with embedded air of different thickness (left).

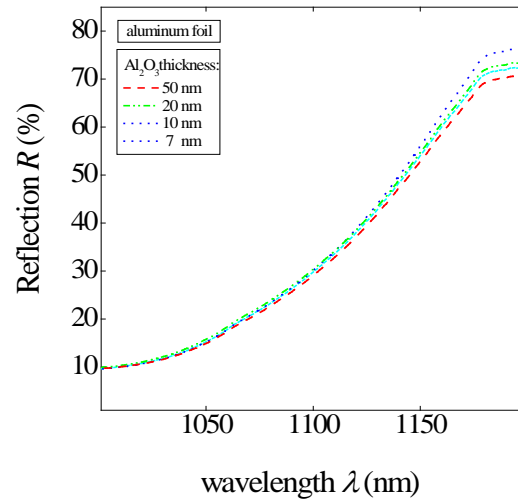
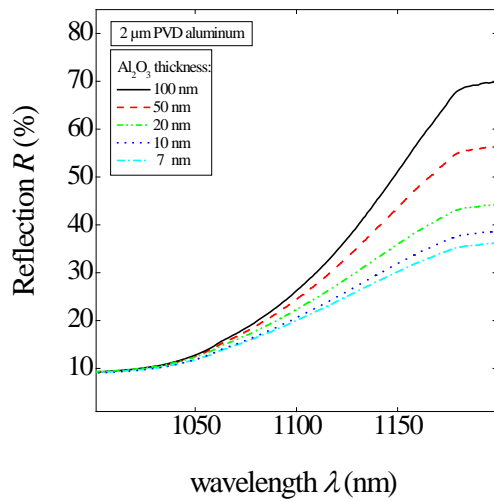


Figure 9: Measured internal reflection on the rear side of samples, passivated with Al₂O₃ layers of different thickness of 6-100 nm in dependence on the metallization processes. On the left side 2 μm PVD aluminum was used, whereas on the right side foil was attached.

6. SOLAR CELLS ON LARGE SUBSTRATES

For further development of the foil approach, its applicability on industrially relevant 156×156 mm² sized multi crystalline (mc) silicon substrates was demonstrated. Concerning this matter a homogeneously application of the foil over the whole area of the substrate is the biggest challenge. Since the so far used provisional attempt does not allow an appropriate foil fixation on larger substrates we planned, constructed and built up a special tool, which rolls the foil onto the wafer and provides a form closed attachment (see Figure 11, left), which leads to homogeneously processed wafers (see figure 11, right). Therewith for the first time, we fabricated twelve 156×156 mm² sized solar cells, seven of them featuring foil metalized rear sides and five reference cells with common PVD metallization.

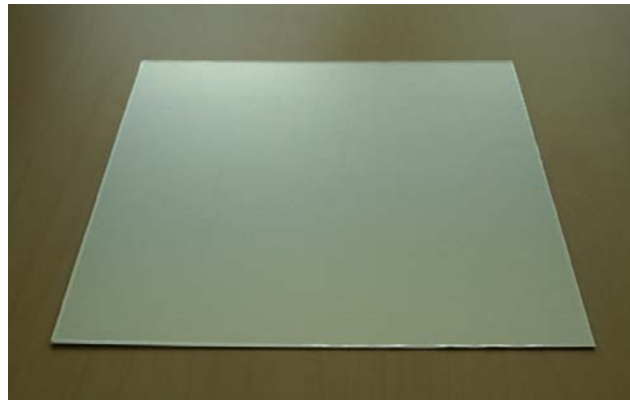
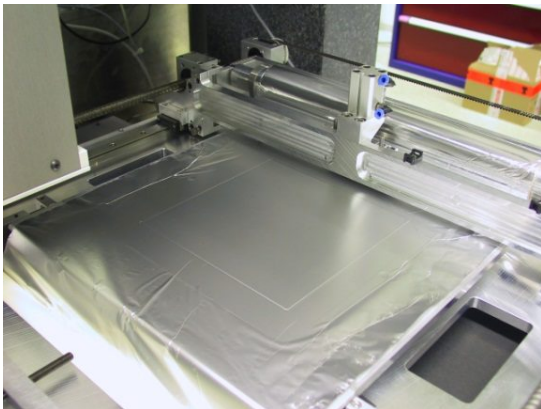


Figure 10: Measured internal reflection on the rear side of samples, passivated with Al₂O₃ layer of different thicknesses between 6-100 nm in dependence on the metallization processes. On the left side 2 μm PVD aluminum was used, whereas on the right side foil was attached.

We used multi crystalline silicon with a base resistivity of $\rho=1.6 \Omega\text{cm}$. The front side covers an emitter with a sheet resistivity of $65 \Omega/\square$, passivated by a PECVD deposited SiN_x layer with standard screen printed contacts. The rear side is passivated by a PECVD deposited stack consisting of 10 nm Al_2O_3 and 90 nm SiO_x . For the metallization 10 μm thin aluminum foil was pinned onto the surface with a multi pulse process similar to process “A” (see section 3). The reference cells received 2 μm PVD metallization on the rear side, which was contacted with a standard single pulse LFC process with adjusted contact pitch. All cells finally underwent a 2 minute lasting forming gas anneal (FGA) at a temperature of 300 °C. The I-V-measurement results are listed in Table 3.

The foil metallized cells show stable values for all I-V parameters leading to an efficiency of 17.1% on average. The V_{oc} could be higher for a passivated cell, but unfortunately only low quality material was used. The J_{sc} value is good compared to a standard al-BSF cell, due to the improved internal reflection of the rear side. The main parameter in this case is the fill factor. Values in the range of 76-78 % are common for solar cells with passivated rear sides and local contacts, since the series resistance is higher compared to standard cells, where the rear side contact covers the full wafer area. These values suggest a homogeneously contacted rear side and hence a stable contacting process over the whole area. Compared to the PVD metallized reference cells, the foil metallized cells show slightly decreased open circuit voltage, which can be caused by increased laser damage due to the multi pulse process. On the other hand the higher fill-factor indicates a slightly higher contact fraction, which can also cause the voltage difference. The short circuit current is a little higher in average, which might be due to the increased internal reflection. The difference in fillfactor is most probably caused by an altered contact fraction.

Table 3: I-V-measurement parameter of seven $156 \times 156 \text{ mm}^2$ sized, multi crystalline solar cells with foil based rear side metallization and of five reference cells with common PVD metallization.

Process		area [cm^2]	V_{oc} [mV]	J_{sc} [mA/ cm^2]	FF [%]	η [%]
Foil	Mean	243.4 ± 0	623 ± 2	35.8 ± 0.2	76.7 ± 0.6	17.1 ± 0.2
	Best cell	243.4	626	35.9	77.4	17.4
PVD	Mean	243.4 ± 0	627 ± 1	35.7 ± 0.2	76.1 ± 0.3	17.0 ± 0.2
	Best cell	243.4	628	36.0	76.5	17.3

Even the high fill-factor of the foil metallized cells points out the successfully contacting and metallization process we investigated the homogeneity by calculating the spatially resolved series resistance R_s from different photo- and electroluminescence images (PL&EL) [10]. These pictures as shown in figure 12, do not reveal any bright regions inside the cell area, where the attachment of the foil or the contacting process did fail.

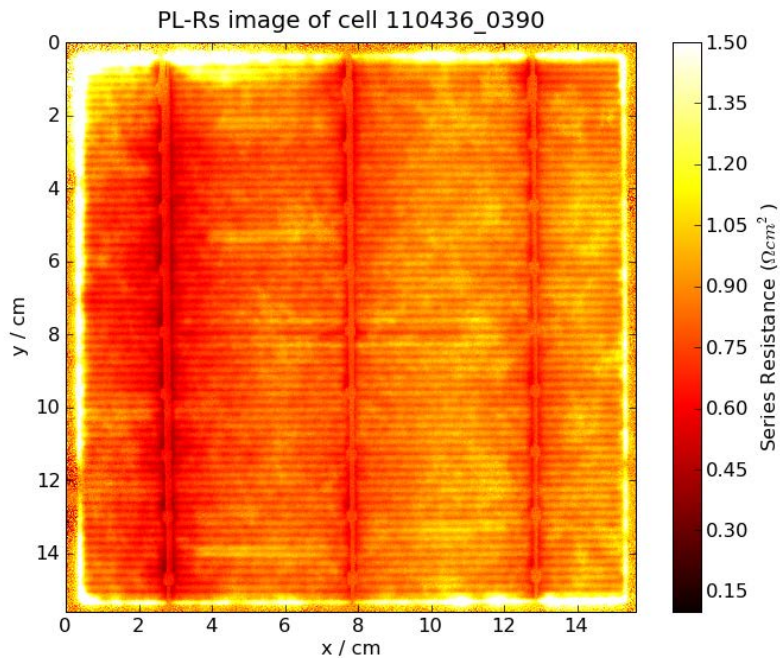


Figure 11: Calculation of the spatially resolved series resistance R_s from different photo- and electroluminescence images.

7. CONCLUSION

In this paper we show that with a simple setup the well-known LFC process can be used to fix aluminum foil successfully and reliably on solar cell rear sides. We have evaluated the influence of different pulse duration regimes, indicating a higher performance regarding the efficiency potential of shorter pulses. We presented results of a solar cell batch, which suggest the equal efficiency potential of this approach compared to those of other more common metallization techniques as screen printing or evaporation, by reaching efficiencies of up to 21.0 %. We carried out simulations regarding the influence and the potential of a thin layer of embedded air between passivation and foil. Thereby we found out, that such a thin air film leads to an increased internal reflectance independently of the passivation layer thickness. We verified these results by means of reflectance measurements on specially processed samples and hence proved the existence of this air gap. Finally we built a special tool to apply the foil on large $156 \times 156 \text{ mm}^2$ wafers. Therewith we processed large, multi-crystalline solar cells with a maximum efficiency of 17.4 %, showing the industrial applicability of this process.

8. ACKNOWLEDGMENTS

The German Ministry for the Environment, Nature Conservation and Nuclear Safety (BMU) is gratefully acknowledged for financially supporting this work within the project: GRIPS (contract number 41V5674). The authors also would like to thank all colleagues at Fraunhofer ISE who have contributed to this paper in general. Special thanks appertain to the ISE PVTEC team for cell processing and I-V measurement and Dirk Maier for carrying out the adhesion tests at the Fraunhofer Module Technology center (MTC).

9. REFERENCES

- [1] E. Schneiderlöchner, R. Preu, R. Lüdemann *et al.*, *Progress in Photovoltaics: Research and Applications* **10** (2002) 29.
- [2] A. W. Blakers, A. Wang, A. M. Milne *et al.*, *Applied Physics Letters* **55** (1989) 1363.
- [3] J. Nekarda, A. Grohe, O. Schultz *et al.*, *Proceedings of the 22nd European Photovoltaic Solar Energy Conference* (2007) 1499.
- [4] A. Grohe, J. Nekarda, and O. Schultz, Germany Patent No. DE 10 2006 044 936 B4 (2008).
- [5] R. H. Cox and H. Strack, *Solid-State Electronics* **10** (1967) 1213.
- [6] M. Hörteis, J. Benick, J. Nekarda *et al.*, *Proceedings of the 35th IEEE Photovoltaic Specialists Conference* (2010) in print.
- [7] M. Hörteis and S.W. Glunz *Progress in Photovoltaics: Research and Applications* **16** (2008) 555.
- [8] A. Aberle, S. Glunz, W. Warta *et al.*, *Proceedings of the 10th European Photovoltaic Solar Energy Conference* (1991) 631.
- [9] R. Brendel, *Proceedings of the 12th European Photovoltaic Solar Energy Conference* (1994) 1339.
- [10] H. Höffler, J. Haunschild, R. Zeidler *et al.*, in *Silicon PV* (Leuven, 2012).